Mechanism of Supported Membrane Disruption by Antimicrobial Peptide Protegrin-1

Kin Lok H. Lam,[†,#] **Yuji Ishitsuka,**[‡,#] **Yishan Cheng,**[§] **Karen Chien,**[§] **Alan J. Waring,**[∥,⊥] **Robert I. Lehrer,**[∥] **and Ka Yee C. Lee*,**[‡,#]

Department of Physics, Department of Chemistry, The Institute for Biophysical Dynamics, and The James Franck Institute, The University of Chicago, Chicago, Illinois 60637, Illinois Mathematics and Science Academy, Aurora, Illinois 60506, Department of Medicine, School of Medicine, University of California at Los Angeles, Los Angeles, California 90095, and Harbor−University of California Los Angeles Medical Center, Torrance, California 90502

While pore formation has been suggested as an important step in the membrane disruption process induced by antimicrobial peptides, membrane pore formation has never been directly visualized. We report on the dynamics of membrane disruption by antimicrobial peptide protegrin-1 (PG-1) on dimyristoyl-*sn*-glycero-phosphocholine-supported bilayer patches obtained via atomic force microscopy. The action of PG-1 is found to be concentration-dependent. At low PG-1 concentrations ($1 < [PG-1] < 4\ \mu g/mL$), the peptide destabilizes the edge of the membrane to form fingerlike structures. At higher concentrations, PG-1 induces the formation of a sievelike nanoporous structure in the membrane. The highest degree of disruption is attained at concentrations $\geq 20\ \mu g/mL$, at which PG-1 disrupts the entire membrane, transforming it into stripelike structures with a well-defined and uniform stripe width. This first direct visualization of these membrane structural transformations helps elucidate the PG-1-induced membrane disruption mechanism.

Introduction

Protegin-1 (PG-1; $M_w = 2154$ Da) is an 18-residue antimicrobial peptide (AMP), representing one of the classes of innate peptides that functions as a protective agent against harmful microorganisms. PG-1 is folded in an antiparallel β-sheet structure,[1−3] and the structure is stabilized by two intramolecular disulfide bonds. Pathogens susceptible to PG-1 include *Escherichia coli* (Gram-negative),[4] *Listeria monocytogenes* (Gram-positive),[4] *Neisseria gonorrheae* (Gram-negative),[5] *Candida albicans* (fungi),[6] and HIV-1 (lipid-coated retrovirus).[7]

The wide range of antimicrobial activity of PG-1 comes from its ability to selectively disrupt the cell membrane of microorganisms. It has been reported that PG-1 forms pores in membranes based on neutron diffraction structural studies of fully hydrated multilamellar systems,[8] experimental evidence for an increase in voltage conductance across planar bilayers,[9] as well as ion leakage from vesicles[10] upon addition of PG-1. However, pore formation has never been directly visualized. There have been previous attempts to monitor topological changes on bilayer surfaces induced by PG-1 using atomic force microscopy (AFM), but no pores were detected, and only increased roughness and undulations were reported.[11,12]

In this work, we present the first direct observation of PG-1-induced structural transformations of supported lipid bilayers

by AFM. The novelty of our methodology is in the use of bilayer patches instead of continuously covered bilayers. The use of bilayer patches provides the bilayers the freedom to expand, thus enabling the efficient insertion of the amphipathic peptide[13] and the subsequent characterization of the lipid−peptide interaction. We have observed an increasing degree of membrane structural disruption with increasing PG-1 concentration over time, progressing from fingerlike instabilities formed at bilayer edges, to the formation of sievelike nanoporous structures in the center of the patches, and finally to the complete disruption of the membrane integrity, resulting in the creation of a network of stripelike structures.

Experimental Methods

1,2-Dimyristoyl-*sn*-glycero-phosphocholine (DMPC) was purchased from Avanti Polar Lipids, Inc. (Alabaster, AL) and used without further purification. High-grade mica was purchased from Ted Pella, Inc. (Redding, CA). Ultrapure water (resistivity $> 18\ M\Omega$ cm) was obtained with a MilliQ (Millipore, Bedford, MA) system. Dulbecco's phosphate-buffered saline (D-PBS), without calcium and magnesium (Invitrogen Co., Carlsbad, CA), was used as the superphase for all of the experiments.

Large unilamellar vesicles were prepared via the freeze−thaw extrusion method.[14] The lipid, dissolved in chloroform, was dried to a thin film under a stream of nitrogen and was left overnight in a vacuum for the solvent to completely evaporate. The lipid film was then hydrated with water and vortexed at 40 °C for 30 min. A typical concentration used during vesicle preparation was 2 mg/mL. After six freeze−thaw cycles, the suspension was extruded through the pores of a polycarbonated membrane (100 nm, Avanti Polar Lipids, Inc.). The size distribution of the resulting vesicles was determined by dynamic light scattering using a model PD2000DLS (Precision Detectors,

* Author to whom correspondence should be addressed. E-mail: kayeelee@uchicago.edu.
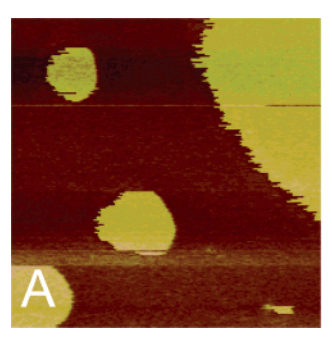† Department of Physics, The University of Chicago.
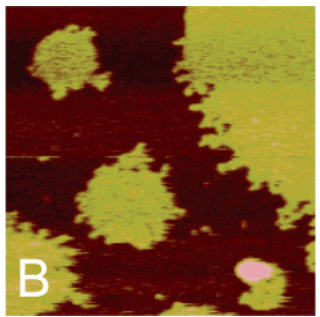‡ Department of Chemistry, The University of Chicago.
The Institute for Biophysical Dynamics and The James Franck Institute, The University of Chicago.
§ Illinois Mathematics and Science Academy.
∥ Department of Medicine, University of California at Los Angeles.
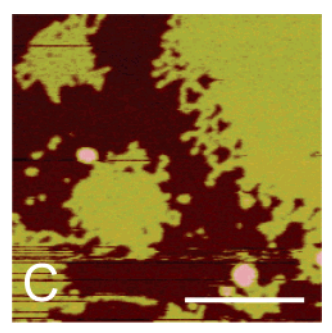⊥ Harbor−University of California at Los Angeles Medical Center.

Figure 1. DMPC bilayer patches (A) before and (B and C) after introducing 2 μg/mL of PG-1 to the superphase. The scale bar is 500 nm. (A) Without PG-1, stable supported bilayer patches maintained smooth boundaries by line tension. (B) After 5 min of incubation in the PG-1 solution, edges were destabilized, and fingerlike structures grew. (C) After 15 min, the destabilization process reached completion, and no further changes were observed.

Franklin, MA) instrument, and the diameter was typically found to be 130 $\pm$ 28 nm.

Supported bilayers were formed using the vesicle fusion method. All experiments were performed under buffer using a commercial fluid cell (Digital Instruments, Santa Barbara, CA). Mica fixed on a stainless steel disk was freshly cleaved and used as a substrate. The mica was immediately hydrated by the buffer solution. Subsequently, 0.4 mL of a 20 μg/mL vesicle solution with 10 mM MgCl$_2$ (Fisher Scientific, ACS grade) was injected into the sample chamber. After 2 min, whereby self-assembled bilayer patches have been formed, the sample chamber was flushed with buffer to remove excess vesicles in suspension. With this concentration, the area coverage of resultant bilayers was measured to be around 20%. All experiments were conducted at 30 $\pm$ 2 °C, a temperature above the critical temperature of DMPC, so that the lipids were in a fluid state throughout the experiments.

Imaging of the unperturbed supported bilayer was then performed in fluid with a MultiMode Nanoscope IIIA scanning probe microscope (Digital Instruments). Cantilevers with oxide-sharpened silicon nitride tips (Digital Instruments), with a nominal spring constant of 0.32 N/m were used in tapping mode with a 160 μm scanner (type J). The drive frequency was between 8 and 9 kHz, and the drive amplitude was between 0.25 and 0.5 V, which corresponded to 5−10 nm. The setpoint was usually between 0.8 and 0.9 of the free amplitude in our experiments. Minimized tapping force was applied during a scan to prevent membrane damage and possible artifacts. A typical scan rate of 1 Hz at a resolution of 256−512 pixels/line was used. Images shown were subjected to a first-order plane-fitting procedure to compensate for sample tilt and, if necessary, to a zeroth-order flattening. The height of the bilayer was obtained by analyzing the distribution of surface heights over a scan (bearing analysis) or the line section of a scan, depending on the nature and the quality of the image. The area of the bilayer was estimated by counting the number of pixels above a certain threshold value determined by analyzing the distribution of surface height over a scan.

After the unperturbed bilayer patches were imaged, a PG-1 solution of a known bulk concentration (C_b) was injected to fully exchange the superphase. A stock PG-1 (1.0 mg/mL) solution was prepared by dissolving the peptide in ultrapure water with 0.01% glacial acetic acid to prevent aggregation and then further diluted to the desired concentration C_b in buffer. The synthesis of PG-1 has been described elsewhere.[2] PG-1 is known to oligomerize in the concentration range of tens of millimolar, but at the concentrations used in this study ($\sim$0.5− 10 μM), the peptide remains monomeric in solution.

Results

Our experiments show that there exists a critical PG-1 concentration below which PG-1 has no impact on the structural integrity of the bilayer patch. This is consistent with the two-state model[15] wherein the peptide only disrupts the membrane when the surface peptide-to-lipid ratio reaches a certain critical value. At a low concentration of 1 μg/mL PG-1, no structural changes were detected on the bilayer patches. At $1 < C_b \leq 4$ μg/mL, structural changes in the bilayer patches started at the edge of the bilayer. At $C_b > 4$ μg/mL, large scale structural transformations of the bilayer patch were observed.

A supported lipid bilayer has been shown to be a good model cell membrane system.[16] The fluidity of the bilayer in terms of its lateral self-diffusion is maintained by an ultrathin layer of water of $\sim$10 Å between the lower leaflet of the bilayer and the substrate.[17] Zwitterionic PC is one of the major lipid components found in eukaryotic cell membranes and is hence chosen as the model lipid system for our study.

In our experiments, free peptides in the bulk were allowed to adsorb to the bilayer until surface partition equilibrium was reached. Under equilibrium conditions, the peptide-to-lipid ratio is directly proportional to C_b.[18] It is also worthy to note that, with the same amount of lipids adsorbed on the mica substrate, the peptide adsorption time scale is independent of C_b.[18] As a result, we expect all our experiments to have a similar equilibrium time scale since the bilayer patch coverage in all experiments was maintained to be roughly the same. Indeed, we found experimentally that all changes induced by PG-1 on DMPC bilayer patches were completed within 15 min of peptide injection. Due to this relatively long time scale for structural transformations to take place, time-lapse AFM measurements have allowed us to capture the dynamics of membrane disruption by PG-1 with high spatial resolution. Scanning of the sample surface started immediately after the introduction of PG-1, and changes in the topology due to various states of peptide association were successfully observed.

Edge Destabilization. For $C_b < 1$ μg/mL, the presence of the peptide did not have any effect on the structure and integrity of the bilayer patch (data not shown). The first sign of structural transformation emerged at the edges of DMPC bilayer patches with $1 < C_b \leq 4$ μg/mL. The adsorption of the peptide to the bilayer patch induced the formation of an extended boundary that was otherwise energetically unfavorable.

Figure 1 shows intact DMPC bilayer patches before and after the introduction of 2 μg/mL PG-1. Neither the mica surface nor the surface of the bilayer patches exhibited any detectable changes in height, and a line scan of the film showed a bilayer
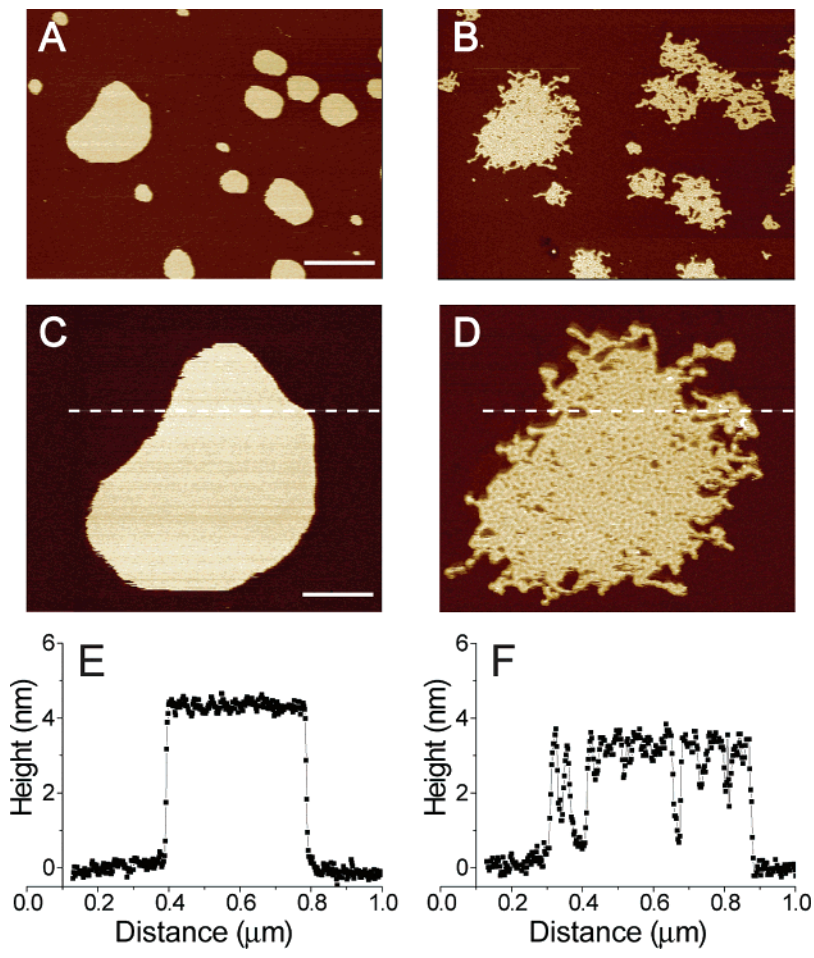
Figure 2. AFM images and line sections of DMPC bilayer patches before and after introducing 10 μg/mL of PG-1 to the superphase. (A) In the absence PG-1, supported bilayer patches maintained lamellar interiors and smooth boundaries; the scale bar is 600 nm. (B) After the introduction of PG-1, both the edge and the interior of the bilayer patches were disrupted, giving rise to a sievelike nanoporous structure. (C and E) Zooming in on one of the bilayer patches reveals a bilayer thickness of 4.4 $\pm$ 0.2 nm when PG-1 is absent. The dashed line in part C indicates the location of the line section shown in part E; the scale bar is 200 nm. (D and F) Introduction of PG-1 to the same patch of lipid bilayer in part C results in the formation of pores in the interior of the membrane and the reduction of the membrane thickness to 3.3 $\pm$ 0.2 nm. The dashed line in part D indicates the location of the line section shown in part F.
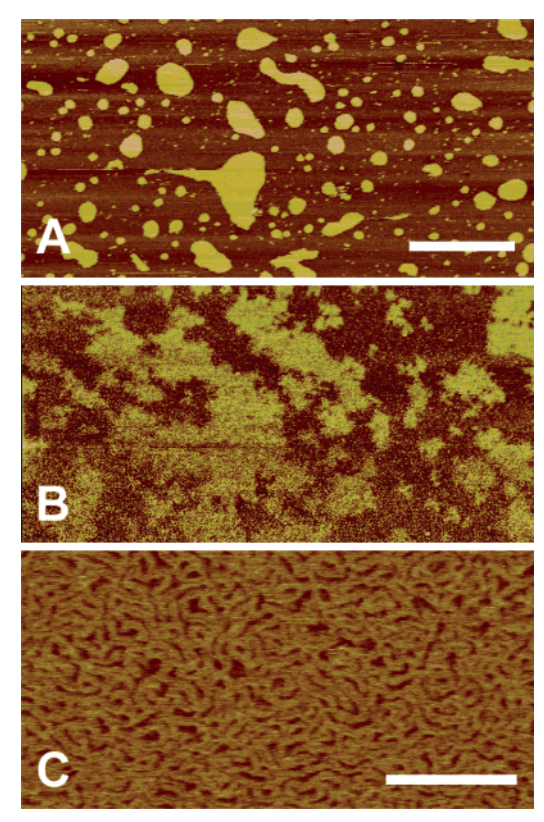
thickness of 4.4 $\pm$ 0.2 nm. However, the lipid bilayer patches, originally with smooth boundaries maintained by line tension (Figure 1A), grew fingerlike contours within 5 min after the superphase was exchanged with 2 μg/mL PG-1 solution (Figure 1B). As shown in Figure 1, while the edges of the bilayer patches were disrupted, the interior remained lamellar and intact. Fifteen minutes after injection of PG-1 solution, the development of fingerlike structures was completed, and no further changes were observed (Figure 1C). Similar edge destabilization has also been observed in bilayer patches incubated with C_b = 2, 3, and 4 μg/mL, and all changes again were completed within 15 min.

Sievelike Nanoporous Structure Formation. When $C_b >$ 4 μg/mL, the interior of the DMPC bilayer patches was transformed into a sievelike nanoporous structure in addition to the development of fingerlike structures around the edges. The formation of such a nanoporous structure has also been observed in bilayer patches with C_b = 5, 6, and 10 μg/mL. Again, all structural changes were completed within 15 min after PG-1 addition, and the sievelike nanoporous structure remained unchanged over time.

Figure 2 shows intact DMPC bilayer patches before and after incubation with a 10 μg/mL PG-1 solution. A sievelike nanoporous structure spanning the entire bilayer (Figures 2B and 2D) was formed from the originally lamellar interior surface (Figures 2A and 2C). The silicon nitride cantilever with an

oxidation sharpened tip used in the experiments has a normal tip radius of about 10 nm. Since the resolution of AFM is limited by the tip radius, the depths of the small pores cannot be fully resolved. High-resolution scans of large pores revealed that the pores actually penetrated all the way to the other side of membrane (Figure 2F). The average thickness of the bilayer (excluding the pores) decreased from 4.4 $\pm$ 0.2 nm before incubation to 3.3 $\pm$ 0.2 nm after PG-1 partitioning equilibrium was reached as shown in Figures 2E and 2F, respectively. Due to the formation of the observed array of pores throughout the bilayer patch and the volume conservation of the lipids in the patch, the total area spanned by the bilayer patch was found to increase. As is obvious from Figure 2D, the edge of the bilayer patch continued to be destabilized by the presence of the peptide, resulting in the formation of fingerlike structures as before.

Complete Membrane Destabilization. At even higher peptide concentrations ($C_b \geq$ 20 μg/mL), the peptide completely disrupted the bilayer structure of the membrane (Figure 3B). Close-up images revealed that the original lamellar membranes turned into a labyrinthine network (Figure 3C). Radial distribution in the Fourier spectrum of the images showed a structural width of 9 nm. The average thickness of the structure was 2.6 $\pm$ 0.3 nm from the substrate, greatly reduced from the original DMPC bilayer thickness of 4.4 $\pm$ 0.2 nm (Figure 3A). As evident in Figures 3B and 3C, the integrity of the original bilayer

Mechanism of Membrane Disruption by Protegrin-1

J. Phys. Chem. B, Vol. 110, No. 42, 2006 **21285**

Figure 3. DMPC bilayer patches (A) before and (B) after introducing 20 μg/mL of PG-1 to the superphase. The bilayer patches became totally destabilized. The scale bar is 1 μm. (C) Closeup of one of the bilayer patch areas revealed the presence of a stripelike structure with an average thickness of 2.6 $\pm$ 0.3 nm and a characteristic width of 9 nm. The scale bar is 100 nm.

was completely destroyed at this concentration. The sievelike nanoporous structure observed at a lower peptide concentration thus represents only an intermediate state along the route of the membrane disruption process of PG-1, though the barrier function of the membrane is already sufficiently compromised by the nanoporous structure attained in this intermediate state.

Discussion and Conclusion

At a given peptide dosage that induces edge instability in the bilayer patches (Figures 1 and 2), the extended contours of the bilayer patches, instead of relaxing back to a more compact shape, remained unchanged over time (observed over several hours) after their initial formation (15 min). The equilibrium shape of a bilayer patch is governed by the competition of two opposing forces: line tension and electrostatic repulsion.[19] Line tension tends to minimize the boundary of the patch, leading to the formation of more compact shapes, while electrostatic repulsive interaction prefers extended domain boundaries. In the absence of the peptide, the line tension is large and outcompetes the dipole−dipole repulsive electrostatic interactions between the lipids in the bilayer. As a result, the bilayer patches attain smooth contours and compact shapes so as to minimize the interface and hence the interfacial energy. The shape relaxation of a supported bilayer patch from some extended shape to a compact one can be slow ($\sim$ 20 min) on a mica surface due to the interaction between the bilayer and the substrate.[14] When the $k_{\mathrm{B}}T$ criterion at 30 °C is used, a line tension ($k_{\mathrm{B}}T/l$) greater than or equal to 10^{-10} N is required for this type of shape relaxation to take place, where k_{B} is Boltzmann's constant, T the room temperature, and $l \approx 10$ Å is the characteristic length between molecules in the bilayer. The

fact that the extended contour of a PG-1-perturbed bilayer patch remains stable without any sign of relaxation for several hours points to two distinct possibilities: (1) the adsorption of PG-1 to the edge of the bilayer patch acts to reduce the line tension of the system to below 10^{-10} N, or (2) the adsorbed cationic PG-1 enhances the electrostatic repulsive interactions of the system, thus favoring the formation of more extended shapes.

In this system, the membrane edge is long ($\sim$1−10 μm) in comparison to the thickness of the membrane ($\sim$4.4 nm), the latter of which is of molecular dimensions. The edge of the bilayer patch can therefore be regarded as a one-dimensional (1D) object: a line. At low C_{b}, adsorption of the peptide to the membrane edge can be described by the 1D counterpart of the Gibbs adsorption equation[20,21]

$$\Gamma_{\mathrm{L}} = -\frac{\mathrm{d}\lambda}{\mathrm{d}\mu} = -(k_{\mathrm{B}}\mathrm{T})^{-1}\left(\frac{\mathrm{d}\lambda}{\mathrm{d}\ln C_{\mathrm{b}}}\right)$$

where Γ_{L} is the line excess or line concentration, λ is the line tension, and $\mu \approx k_{\mathrm{B}}T \ln C_{\mathrm{b}}$ is the chemical potential. According to this, the line tension decreases as the number of adsorbed peptide molecules increases. The extended domain shape in the PG-1-perturbed bilayer patches therefore suggests that PG-1 is line-active and its adsorption to the edge of the bilayer patch lowers its line tension ($\Gamma_{\mathrm{L}} > 0$).

As the PG-1 molecules bear a net positive charge, their adsorption to the bilayer surface enhances the electrostatic repulsive interactions of the system. As shown by Lord Rayleigh,[22] the spherical shape of a freely suspended liquid drop becomes unstable when the overall charge of the drop is greater than some threshold value. As long as the electrostatics are not perfectly screened by electrolytes, one may similarly think of our system of two-dimensional (2D) bilayer patches as gradually being charged by the adsorbed peptides, and the smooth boundaries of the patches are rendered unstable when enough peptides have been adsorbed, making the electrostatic repulsive interaction dominant over the line tension effect. The edge instability observed here in our model 2D system is also reminiscent of the microvilli formation previously captured by electron microscopy in *E. coli* when subjected to PG-1.[13]

The results reported here strongly suggest that PG-1 is line-active and that the edges of the bilayer patches are more susceptible to PG-1 disruption in comparison to the lamellar region of the patches. The long-term stability of the structures obtained also suggests that once inserted the peptide remains bound to the membrane. Although PG-1 is well-known to target anionic membranes, our work shows that it is disruptive toward zwitterionic membranes at high enough peptide concentrations. As evident from our data, there exists critical PG-1 concentrations, above each of which a different kind of structural transformation of the bilayer patches can take place. In contrast to previous studies where the formation of pores at the membrane surface can only be implicated, our findings provide the first direct visualization of the membrane disruption process by PG-1, from edge destabilization, to the formation of a sievelike nanoporous structure, and finally to the complete disruption and transformation of the lamellar membrane to a network of stripelike structures at even higher peptide concentrations. This suggests that pore formation may only be an intermediate state along the path of membrane destabilization by PG-1.

Preliminary results on bilayer patches containing anionic lipids reveal analogous topological changes to those seen in the DMPC patches reported here but with a lower PG-1 dose requirement. This points to a similar membrane disruption

21286 *J. Phys. Chem. B, Vol. 110, No. 42, 2006*

Lam et al.

pathway employed by PG-1 for both zwitterionic and anionic membranes. Further qualitative investigation of the structural transformation as well as the effects of bilayer lipid compositions and charge screening will be conducted soon.

References and Notes

(1) Roumestand, C.; Louis, V.; Aumelas, A.; Grassy, G.; Calas, B.; Chavanieu, A. *FEBS Lett.* **1998**, *421*, 263.

(2) Fahrner, R. L.; Dieckmann, T.; Harwig, S. S.; Lehrer, R. I.; Eisenberg, D.; Feigon, J. *Chem. Biol.* **1996**, *3*, 543.

(3) Buffy, J. J.; Waring, A. J.; Hong, M. *J. Am. Chem. Soc.* **2005**, *127*, 4477.

(4) Kokryakov, V. N.; Harwig, S. S.; Panyutich, E. A.; Shevchenko, A. A.; Aleshina, G. M.; Shamova, O. V.; Korneva, H. A.; Lehrer, R. I. *FEBS Lett.* **1993**, *327*, 231.

(5) Qu, X. D.; Harwig, S. S.; Oren, A. M.; Shafer, W. M.; Lehrer, R. I. *Infect. Immun.* **1996**, *64*, 1240.

(6) Cho, Y.; Turner, J. S.; Dinh, N. N.; Lehrer, R. I. *Infect. Immun.* **1998**, *66*, 2486.

(7) Tamamura, H.; Murakami, T.; Horiuchi, S.; Sugihara, K.; Otaka, A.; Takada, W.; Ibuka, T.; Waki, M.; Yamamoto, N.; Fujii, N. *Chem. Pharm. Bull.* **1995**, *43*, 853.

(8) Yang, L.; Weiss, T. M.; Lehrer, R. I.; Huang, H. W. *Biophys. J.* **2000**, *79*, 2002.

(9) Mangoni, M. E.; Aumelas, A.; Charnet, P.; Roumestand, C.; Chiche, L.; Despaux, E.; Grassy, G.; Calas, B.; Chavanieu, A. *FEBS Lett.* **1996**, *383*, 93.

(10) Sokolov, Y.; Mirzabekov, T.; Martin, D. W.; Lehrer, R. I.; Kagan, B. L. *Biochim. Biophys. Acta* **1999**, *1420*, 23.

(11) Zhang, L.; Vidu, R.; Waring, A. J.; Lehrer, R. I.; Longo, M. L.; Stroeve, P. *Langmuir* **2002**, *18*, 1318.

(12) Carmichael, M.; Vidu, R.; Maksumov, A.; Palazoglu, A.; Stroeve, P. *Langmuir* **2004**, *20*, 11557.

(13) Gidalevitz, D.; Ishitsuka, Y. J.; Muresan, A. S.; Konovalov, O.; Waring, A. J.; Lehrer, R. I.; Lee, K. Y. C. *Proc. Natl. Acad. Sci. U.S.A.* **2003**, *100*, 6302.

(14) Muresan, A. S.; Lee, K. Y. C. *J. Phys. Chem. B* **2001**, *105*, 852.

(15) Huang, H. W. *Biochemistry* **2000**, *39*, 8347.

(16) Sackmann, E. *Science* **1996**, *271*, 43.

(17) Groves, J. T.; Ulman, N.; Cremer, P. S.; Boxer, S. G. *Langmuir* **1998**, *14*, 3347.

(18) Schwarz, G. *Biochimie* **1989**, *71*, 1.

(19) Lee, K. Y. C.; Mcconnell, H. M. *J. Phys. Chem.* **1993**, *97*, 9532.

(20) Chen, P. *Colloids Surf., A* **2000**, *161*, 23.

(21) Puech, P. H.; Borghi, N.; Karatekin, E.; Brochard-Wyart, F. *Phys. Rev. Lett.* **2003**, *90*.

(22) Rayleigh, L. *Philos. Mag.* **1882**, *14*, 184.